

Spectral evolution and the onset of the X-ray GRB afterglow

P.A. Evans, J.P. Osborne, R. Willingale and P.T. O'Brien

X-ray and Observational Astronomy Group, Dept. of Physics & Astronomy, University of Leicester, Leicester, UK, LE1 7RH

Abstract. Based on light curves from the Swift Burst Analyser, we investigate whether a ‘dip’ feature commonly seen in the early-time hardness ratios of Swift-XRT data could arise from the juxtaposition of the decaying prompt emission and rising afterglow. We are able to model the dip as such a feature, assuming the afterglow rises as predicted by Sari and Piran [1]. Using this model we measure the initial bulk Lorentz factor of the fireball. For a sample of 23 GRBs we find a median value of $\Gamma_0 = 225$, assuming a constant-density circumburst medium; or $\Gamma_0 = 93$ if we assume a wind-like medium.

Keywords: Gamma Ray Bursts

PACS: 98.70.Rz, 95.75.Wx

INTRODUCTION

The early Swift-XRT observations of GRBs have long been seen to exhibit spectral evolution ([2]; [3]). A feature seen in a number of GRBs is a ‘dip’ in the hardness ratio (i.e. a softening followed by a hardening; see Fig. 1a) at the end of the steep decay phase. The Swift Burst Analyser light curves ([4]), which are in units of the intrinsic (i.e. unabsorbed) flux and account for spectral evolution, suggest that this may correspond to the ‘turn-on’ on the X-ray afterglow (Fig. 1b).

The rise of the afterglow was considered by [1], who predicted that it rise as t^2 until some time t_p at which point it peaks and begins to decay. This time t_p corresponds to the deceleration radius: the radius at which the rest mass energy of the material swept up by the fireball equals the energy of the fireball. From this one can determine the bulk Lorentz factor at the deceleration radius of the fireball (e.g. [1]; [5]).

$$\frac{\Gamma_0}{2} = \left(\frac{3E_{\text{iso}} [1+z]^3}{32\pi n m_p c^5 \eta t_p^3} \right)^{\frac{1}{8}} \quad (1)$$

Where E_{iso} is the isotropic equivalent energy output of the GRB, n is the number density of the circumburst medium, and η is the radiative efficiency of the fireball.

This assumes that the density is constant, i.e. the GRB is in an ISM-like environment. If we instead assume that the environment is wind-like (i.e. $\rho \propto r^{-2}$) we find:

$$\frac{\Gamma_0}{2} = \left(\frac{E_{\text{iso}} [1+z]}{8\pi A m_p c^3 \eta t_p} \right)^{\frac{1}{4}} \quad (2)$$

where A is the density normalisation. Following Molinari et al. we assume $\eta = 0.2$, $n = 1 \text{ cm}^{-3}$ and $A = 3 \times 10^{35} \text{ cm}^{-1}$; noting that dependence on these unknowns is weak.

In this paper we will therefore consider whether the X-ray hardness ratio dip can be used to constrain the rise of the X-ray afterglow and hence the initial bulk Lorentz factor, given the Sari & Piran model. It should be noted that the presence of a plateau phase in X-ray data is often interpreted as a sign of continued energy injection into the fireball in some form or other (e.g. [6]). It is likely that this will modify the fireball dynamics somewhat, however since the rate of energy injection is much lower than the rate of energy output in the prompt GRB, we believe we can safely disregard this effect.

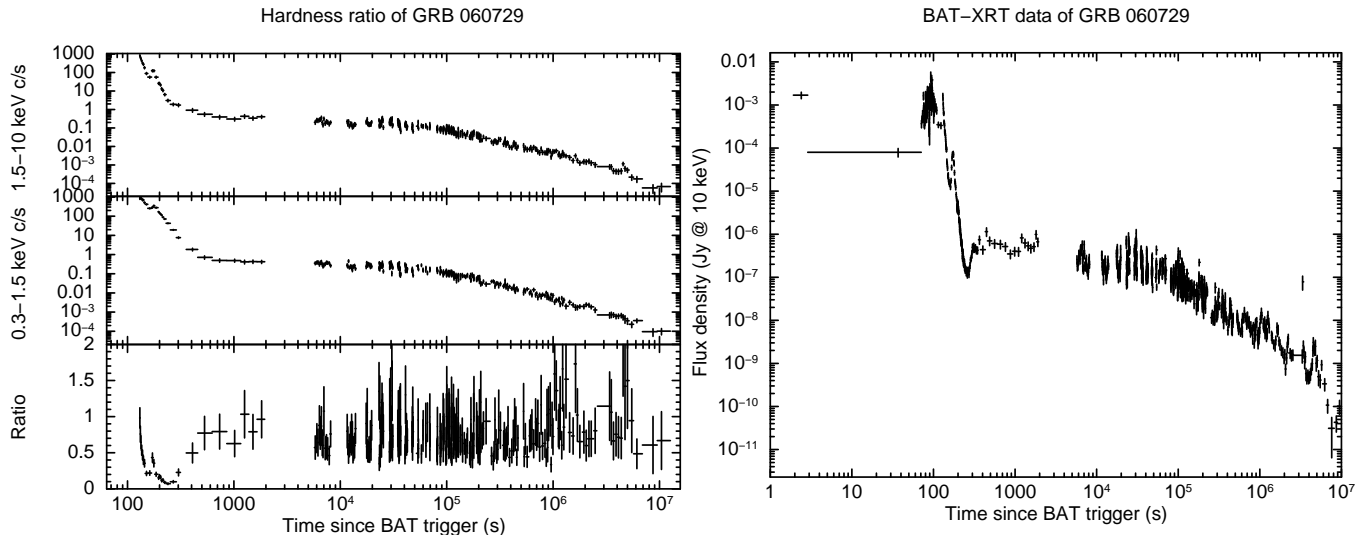


FIGURE 1. The $(1.5-10)/(0.3-1.5)$ keV hardness ratio of GRB 060729 (left panel), showing the ‘dip’ feature around 100–200 s after the trigger. The reconstructed 10 keV flux density light curve from the Burst Analyser light curve (right panel) – which accounts for this spectral evolution – shows a feature at this same time, suggestive of the overlap of the decaying prompt emission and rising afterglow.

MODEL FITTING

To investigate whether the hardness ratio dip can indeed be caused by the rise of the afterglow, we fit the hard (1.5–10 keV) and soft (0.3–10 keV) XRT band data from the XRT light curve repository ([7], [8]) simultaneously. We fit two components: the first models the decaying prompt emission which we parameterise with the pulse model described by Willingale et al. (2005); the hardness ratio of this component decreases (i.e. softens) as a power-law. The second component model is the afterglow, which we treat as spectrally invariant. This component is zero until some time t_a at which the afterglow ‘starts’, thereafter it rises as t^2 until t_p whereafter it breaks to a generic $t^{-\alpha}$ decay.

We do not fit the entire light curve, since we are only interested in the transition from the prompt to afterglow emission. If the afterglow light curve shows evidence for a further break after that referred to above, the data after this break are excluded from the fit. Similarly any breaks or flares which occur before the prompt emission follows a single power-law are excluded; if the burst shows none of these features the entire dataset is fitted. Example fits are shown in Fig. 2.

RESULTS

We identified GRBs with known redshift, a clear dip feature in the hardness ratio, no flares close to or overlapping the dip, and where Swift observed throughout the dip feature. This gave an list of 23 GRBs. Histograms of the initial Lorentz factors determined from these fits are given in Fig. 3. For an ISM-like environment the median value is 225, with most values being above 100, in agreement with measurements in the literature (e.g. [5], [9], [10], [11]). On the other hand, if we assume a wind-like environment the median value of the initial Lorentz factor is only 93, and is below 50 for several bursts; this is close to the limit imposed by the compactness problem and may suggest that these GRBs cannot have occurred in a wind-like environment. We note that all of our values are well below $\Gamma_0 = 1000$, which has been proposed as a lower limit on the bulk Lorentz factor given the GeV emission detected by Fermi-LAT (e.g. [12]). However none of the GRBs in our sample are those which were also observed by the LAT. Also note that [13] and Haoscoët et al. (these proceedings) have argued that GeV photons can escape from a Fireball with bulk Lorentz factors substantially below 1000.

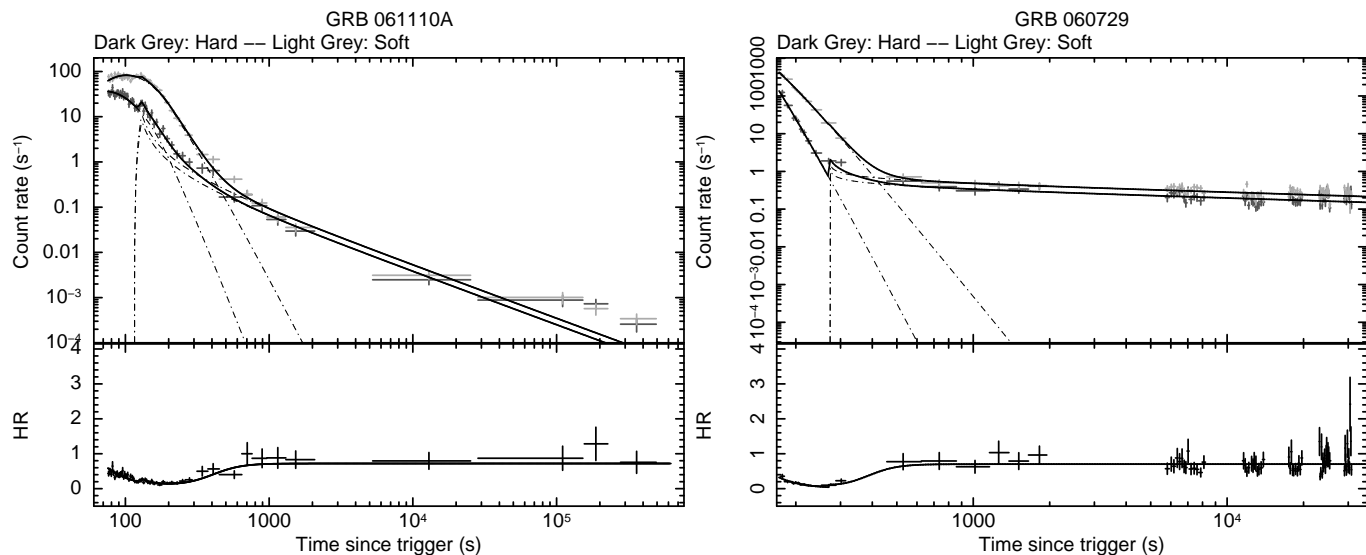


FIGURE 2. Examples fits. The dot-dashed lines show the individual components. The top panel shows the fitted data, the bottom panel the hardness ratio. The latter is not fitted, but is calculated from the top panel, and is shown to illustrate how the model reproduces the dip feature. Left panel: GRB 061110A. Right panel: GRB 060729

CONCLUSIONS

We have shown that a dip feature seen in the X-ray hardness ratios of GRBs at the end of the steep decay phase can be interpreted as the turn-on of the X-ray afterglow, which rises in accordance with the predictions of [1]. By modelling this rise we have determined the initial bulk Lorentz factor for 23 GRBs, finding a median value of 225 assuming an ISM-like circumburst medium, or 93 for a wind-like medium.

REFERENCES

1. R. Sari, and T. Piran, *ApJ* **520**, 641–649 (1999), [arXiv:astro-ph/9901338](#).
2. R. L. C. Starling, P. M. Vreeswijk, S. L. Ellison, E. Rol, K. Wiersema, A. J. Levan, N. R. Tanvir, R. A. M. J. Wijers, C. Tadhunter, J. Rodriguez Zaurin, R. M. Gonzalez Delgado, and C. Kouveliotou, *A&A* **442**, L21–L24 (2005), [arXiv:astro-ph/0508237](#).
3. N. R. Butler, and D. Kocevski, *ApJ* **663**, 407–419 (2007), [arXiv:astro-ph/0612564](#).
4. P. A. Evans, R. Willingale, J. P. Osborne, P. T. O’Brien, K. L. Page, C. B. Markwardt, S. D. Barthelmy, A. P. Beardmore, D. N. Burrows, C. Pagani, R. L. C. Starling, N. Gehrels, and P. Romano, *A&A* **519**, A102+ (2010), 1004.3208.
5. E. Molinari, S. D. Vergani, D. Malesani, S. Covino, P. D’Avanzo, G. Chincarini, F. M. Zerbi, L. A. Antonelli, P. Conconi, V. Testa, G. Tosti, F. Vitali, F. D’Alessio, G. Malaspina, L. Nicastro, E. Palazzi, D. Guetta, S. Campana, P. Goldoni, N. Masetti, E. J. A. Meurs, A. Monfardini, L. Norci, E. Pian, S. Piranomonte, D. Rizzuto, M. Stefanon, L. Stella, G. Tagliaferri, P. A. Ward, G. Ihle, L. Gonzalez, A. Pizarro, P. Sinclair, and J. Valenzuela, *A&A* **469**, L13–L16 (2007), [arXiv:astro-ph/0612607](#).
6. B. Zhang, Y. Z. Fan, J. Dyks, S. Kobayashi, P. Mészáros, D. N. Burrows, J. A. Nousek, and N. Gehrels, *ApJ* **642**, 354–370 (2006), [arXiv:astro-ph/0508321](#).
7. P. A. Evans, A. P. Beardmore, K. L. Page, L. G. Tyler, J. P. Osborne, M. R. Goad, P. T. O’Brien, L. Vetere, J. Racusin, D. Morris, D. N. Burrows, M. Capalbi, M. Perri, N. Gehrels, and P. Romano, *A&A* **469**, 379–385 (2007), 0704.0128.
8. P. A. Evans, A. P. Beardmore, K. L. Page, J. P. Osborne, P. T. O’Brien, R. Willingale, R. L. C. Starling, D. N. Burrows, O. Godet, L. Vetere, J. Racusin, M. R. Goad, K. Wiersema, L. Angelini, M. Capalbi, G. Chincarini, N. Gehrels, J. A. Kennea, R. Margutti, D. C. Morris, C. J. Mounford, C. Pagani, M. Perri, P. Romano, and N. Tanvir, *MNRAS* **397**, 1177–1201 (2009), 0812.3662.
9. R. Xue, Y. Fan, and D. Wei, *A&A* **498**, 671–676 (2009), 0902.2613.
10. P. Kumar, E. McMahon, A. Panaitescu, R. Willingale, P. O’Brien, D. Burrows, J. Cummings, N. Gehrels, S. Holland, S. B. Pandey, D. vanden Berk, and S. Zane, *MNRAS* **376**, L57–L61 (2007), [arXiv:astro-ph/0702319](#).
11. A. Melandri, S. Kobayashi, C. G. Mundell, C. Guidorzi, A. de Ugarte Postigo, G. Pooley, M. Yoshida, D. Bersier, A. J. Castro-Tirado, M. Jelínek, A. Gomboc, J. Gorosabel, P. Kubánek, M. Bremer, J. M. Winters, I. A. Steele, I. de Gregorio-Monsalvo, R. J. Smith, D. García-Appadoo, A. Sota, and A. Lundgren, *ApJ* **723**, 1331–1342 (2010), 1009.4361.

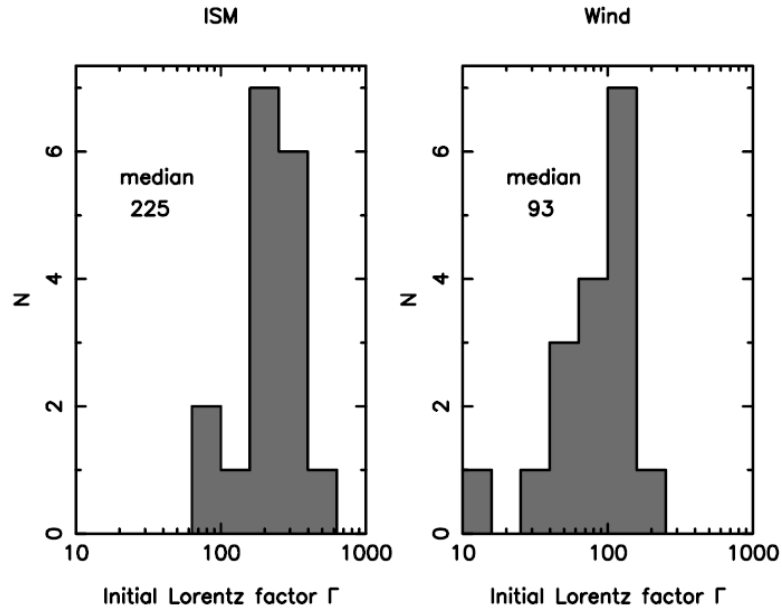


FIGURE 3. The distribution of fireball initial bulk Lorentz factors determined from our fitting, for a constant-density (left) or wind-like (right) circumburst medium.

12. A. A. Abdo, M. Ackermann, M. Ajello, K. Asano, W. B. Atwood, M. Axelsson, L. Baldini, J. Ballet, G. Barbiellini, M. G. Baring, D. Bastieri, K. Bechtol, R. Bellazzini, B. Berenji, P. N. Bhat, E. Bissaldi, R. D. Blandford, E. D. Bloom, E. Bonamente, A. W. Borgland, A. Bouvier, J. Bregeon, A. Brez, M. S. Briggs, M. Brigida, P. Bruel, J. M. Burgess, D. N. Burrows, S. Buson, G. A. Caliandro, R. A. Cameron, P. A. Caraveo, J. M. Casandjian, C. Cecchi, Ö. Çelik, A. Chekhtman, C. C. Cheung, J. Chiang, S. Ciprini, R. Claus, J. Cohen-Tanugi, L. R. Cominsky, V. Connaughton, J. Conrad, S. Cutini, V. d'Elia, C. D. Dermer, A. de Angelis, F. de Palma, S. W. Digel, B. L. Dingus, E. d. C. e. Silva, P. S. Drell, R. Dubois, D. Dumora, C. Farnier, C. Favuzzi, S. J. Fegan, J. Finke, G. Fishman, W. B. Focke, P. Fortin, M. Frailis, Y. Fukazawa, S. Funk, P. Fusco, F. Gargano, N. Gehrels, S. Germani, G. Giavitto, B. Giebels, N. Giglietto, F. Giordano, T. Glanzman, G. Godfrey, A. Goldstein, J. Granot, J. Greiner, I. A. Grenier, J. E. Grove, L. Guillemot, S. Guiriec, Y. Hanabata, A. K. Harding, M. Hayashida, E. Hays, D. Horan, R. E. Hughes, M. S. Jackson, G. Jóhannesson, A. S. Johnson, R. P. Johnson, W. N. Johnson, T. Kamae, H. Katagiri, J. Kataoka, N. Kawai, M. Kerr, R. M. Kippen, J. Knödlseeder, D. Kocevski, N. Komin, C. Kouveliotou, M. Kuss, J. Lande, L. Latronico, M. Lemoine-Goumard, F. Longo, F. Loparco, B. Lott, M. N. Lovellette, P. Lubrano, G. M. Madejski, A. Makeev, M. N. Mazziotta, S. McBreen, J. E. McEnery, S. McGlynn, C. Meegan, P. Mészáros, C. Meurer, P. F. Michelson, W. Mitthumsiri, T. Mizuno, A. A. Moiseev, C. Monte, M. E. Monzani, E. Moretti, A. Morselli, I. V. Moskalenko, S. Murgia, T. Nakamori, P. L. Nolan, J. P. Norris, E. Nuss, M. Ohno, T. Ohsugi, N. Omodei, E. Orlando, J. F. Ormes, W. S. Paciesas, D. Paneque, J. H. Panetta, V. Pelassa, M. Pepe, M. Pesce-Rollins, V. Petrosian, F. Piron, T. A. Porter, R. Preece, S. Rainò, R. Rando, A. Rau, M. Razzano, S. Razzaque, A. Reimer, O. Reimer, T. Reposeur, S. Ritz, L. S. Rochester, A. Y. Rodriguez, P. W. A. Roming, M. Roth, F. Ryde, H. Sadrozinski, D. Sanchez, A. Sander, P. M. Saz Parkinson, J. D. Scargle, T. L. Schalk, C. Sgrò, E. J. Siskind, P. D. Smith, P. Spinelli, M. Stamatikos, F. W. Stecker, G. Stratta, M. S. Strickman, D. J. Suson, C. A. Swenson, H. Tajima, H. Takahashi, T. Tanaka, J. B. Thayer, J. G. Thayer, D. J. Thompson, L. Tibaldo, D. F. Torres, G. Tosti, A. Tramacere, Y. Uchiyama, T. Uehara, T. L. Usher, A. J. van der Horst, V. Vasileiou, N. Vilchez, V. Vitale, A. von Kienlin, A. P. Waite, P. Wang, C. Wilson-Hodge, B. L. Winer, K. S. Wood, R. Yamazaki, T. Ylinen, and M. Ziegler, *ApJ* **706**, L138–L144 (2009), 0909.2470.
13. X. Zhao, Z. Li, and J. Bai, *ApJ* **726**, 89+ (2011), 1005.5229.